ISA Transactions 63 (2016) 377–386

Contents lists available at ScienceDirect

ISA Transactions

journal homepage: www.elsevier.com/locate/isatrans

Composite disturbance rejection control based on generalized extended state observer

Yanjun Zhang, Jun Zhang, Lu Wang, Jianbo Su *

Department of Automation; Key Laboratory of System Control and Information Processing, Ministry of Education, Shanghai Jiao Tong University, Shanghai 200240, PR China

ARTICLE INFO

Article history:
Received 24 January 2016
Received in revised form
22 March 2016
Accepted 31 March 2016
Available online 26 April 2016
This paper was recommended for publication by Dr. Jeff Pieper.

Keywords:
Generalized extended state observer (ESO)
Disturbance rejection
System reconstruction
Aircraft control

ABSTRACT

Traditional extended state observer (ESO) design method does not focus on analysis of system reconstruction strategy. The prior information of the controlled system cannot be used for ESO implementation to improve the control accuracy. In this paper, composite disturbance rejection control strategy is proposed based on generalized ESO. First, the disturbance rejection performance of traditional ESO is analyzed to show the essence of the reconstruction strategy. Then, the system is reconstructed based on the equivalent disturbance model. The generalized ESO is proposed based on the reconstructed model, while convergence of the proposed ESO is analyzed along with the outer loop feedback controller. Simulation results on a second order mechanical system show that the proposed generalized ESO can deal with the external disturbance with known model successfully. Experiment of attitude tracking task on an aircraft is also carried out to show the effectiveness of the proposed method.

1. Introduction

System uncertainties, such as parameters perturbation, unmodeled dynamics, external disturbances, and sensor noise, will have great influence on the performance of a control system, even cause instability. It is not an easy work to design a controller which guarantees both disturbance rejection and tracking performance simultaneously with complicated uncertainties. Thus, composite disturbance rejection methodology with both outer loop controller and inner loop observer has been widely concerned [1]. For the composite disturbance rejection control system, the control accuracy is largely determined by the estimation accuracy of inner loop observer. There have been several observer design approaches investigated so far, such as disturbance observer [2], extended state observer (ESO) [3], unknown input observer [4], perturbation observer [5], equivalent input observer [6], sliding mode observer [7], and fuzzy observer [8–10]. Among these works, ESO needs the least prior information, even if the relative order of the plant is unknown [11]. On the other hand, comparing with the output observers, ESO can estimate not only the equivalent disturbance, but also the internal system states. Thus, state feedback controller can be designed for ESO based control system. According to these advantages, ESO based control, also known as active disturbance rejection control (ADRC), has been widely explored in recent years. It is reported that ESO has been employed in many successful applications, such as uncalibrated visual servoing [12], flight control [13], vibration control [14], power electronics [15], motor control [16]. In addition, various theoretical analyses have been explored based on ESO, such as Lyapunov stability analysis [17], parameter tuning strategy [18], and generalized ESO design for system of mismatched uncertainties [19].

As for the ESO based control structure, observation performance will largely determine the control performance of closed-loop system. Thus, various results on convergence analysis have appeared. For some researches, it is assumed that the change rate of uncertainty is bounded [13,15,19,20]. Then the estimation error of the ESO remains bounded, and its upper bound decreases monotonously when increasing the bandwidth of the observer. By introducing assumption on the system uncertainty, Lyapunov stability analysis of both nonlinear ESO is proposed in [17]. However, the above analysis is only proposed for traditional ESO design.

Despite the theoretical tools for convergence analysis, the specific disturbance rejection performance is rarely investigated, especially for different kinds of time-varying disturbances. It can be obtained in [21] that typical ESO offers asymptotic convergence of estimation for constant disturbance. However, time-varying disturbance, which is widely existing in practice, cannot be estimated by traditional ESO thoroughly [21]. Thus, it is important to explore the observer design methodology against time-varying disturbance for better disturbance rejection performance.

* Corresponding author.
E-mail address: jbsu@sjtu.edu.cn (J. Su).

http://dx.doi.org/10.1016/j.isatra.2016.03.021
0019-0578/

In [22], the generalized ESO with high order is investigated, showing that it improves in the tracking of fast time-varying sinusoidal disturbances. From the results, it can be seen that the high order ESO can improve the estimation accuracy of sinusoidal external disturbances more or less. However, there still exists a periodic estimation error, which will in turn decrease the control accuracy of the closed-loop system [22]. According to internal model principle, the observer cannot reject the disturbance exactly unless the disturbance dynamics is embedded into the observer. In this paper, comparing with the high order ESO [22], the internal model principle is applied for generalized ESO implementation.

This paper devotes to increase the estimating accuracy of ESO against time-varying external disturbances. The definition of extended state for ESO is essentially the reconstruction for the controlled object. However, the existing researches only focus on the performance of ESO with different orders, while the prior information of system uncertainties cannot be further used for ESO implementation. Thus, we first analyze the reconstruction strategy of traditional ESO, and its limitation in dealing with time-varying disturbances is pointed out. To solve this problem, the system is reconstructed based on the model of the system uncertainties, and then the generalized ESO is proposed. At last, stability of the closed-loop system is analyzed along with the outer loop controller.

The rest of this paper is organized as follows. In Section 2, disturbance rejection performance of the traditional ESO is analyzed to show its limitations when dealing with time-varying disturbance. In Section 3, the controlled object is reconstructed by taking the disturbance model into account. Thus, a generalized ESO strategy for composite disturbance rejection is proposed. In Sections 4 and 5, both simulation and experiment are carried out to verify the effectiveness of the proposed strategy, followed by Conclusions in Section 6.

2. Problem statement

2.1. Traditional ESO

Consider the following uncertain single-input single-output (SISO) system, depicted by [17]:

$$\begin{cases} \dot{x}_1 = x_2 \\ \dot{x}_2 = x_3 \\ \cdots \\ \dot{x}_n = f(t, x_1, x_2, \ldots, x_n) + w(t) + u(t) \\ y(t) = x_1, \end{cases} \tag{1}$$

where $x_1, x_2, \ldots, x_n$ are the system states, u and y are the control input and output, respectively. w is the external disturbance, $f(\cdot)$ is the equivalent disturbance caused by both internal uncertainty and external disturbance.

In typical ESO an augmented variable $x_{n+1} \triangleq f(t, x, x_1, \ldots, x_n) + w(t)$ is introduced, such that the system can be reconstructed as:

$$\begin{cases} \dot{\boldsymbol{x}} = A\boldsymbol{x} + Bu + Eh \\ y = C\boldsymbol{x}, \end{cases} \tag{2}$$

where

$$A = \begin{bmatrix} 0 & 1 & 0 & \cdots & 0 \\ 0 & 0 & 1 & \cdots & 0 \\ \vdots & \vdots & \vdots & \ddots & \vdots \\ 0 & 0 & 0 & \cdots & 1 \\ 0 & 0 & 0 & \cdots & 0 \end{bmatrix}_{(n+1)\times(n+1)}, \quad B = \begin{bmatrix} 0 \\ 0 \\ \vdots \\ 1 \\ 0 \end{bmatrix}_{(n+1)\times 1}, \quad E = \begin{bmatrix} 0 \\ 0 \\ \vdots \\ 0 \\ 1 \end{bmatrix}_{(n+1)\times 1},$$

$$C = [1\ 0\ \cdots\ 0\ 0]_{1\times(n+1)},$$

$$h = \frac{\mathrm{d}f(t, x_1, x_2, \ldots, x_n(t))}{\mathrm{d}t} + \frac{\mathrm{d}w(t)}{\mathrm{d}t}.$$

Then the linear ESO can be designed as follows:

$$\begin{cases} \dot{\boldsymbol{z}} = A\boldsymbol{z} + Bu + L(y - \hat{y}) \\ \hat{y} = C\boldsymbol{z}, \end{cases} \tag{3}$$

where $\boldsymbol{z} \in \mathbb{R}^{n+1}$, $L = \begin{bmatrix} l_1 & l_2 & \cdots & l_{n+1} \end{bmatrix}^{\mathrm{T}}$ such that all the roots of $s^{n+1} + l_1 s^n + \cdots + l_n s + l_{n+1} = 0$ are located at the right half s-plane. The selection of the observer gain is investigated in [18] based on bandwidth theory, which has been widely concerned in practice.

2.2. Disturbance rejection performance analysis

By introducing the Laplace transformation upon Eqs. (2) and (3), we get

$$z_{n+1} = H(s)x_{n+1}, \quad H(s) = \frac{l_{n+1}}{s^{n+1} + l_1 s^n + \cdots + l_n s + l_{n+1}}. \tag{4}$$

where $H(s)$ is an equivalent filter in the disturbance rejection structure. It is clearly that the control accuracy of the closed-loop system relies on the accuracy of the estimated disturbance z_{n+1}.

Assume that $\lim_{t\to\infty} x_i(t) = 0, i = 1, \ldots, n$. Without loss of generality, it is assumed that

$$\lim_{t\to\infty} f(t, x_1, x_2, \ldots, x_n) = 0.$$

Then we get

$$\begin{aligned} \lim_{t\to\infty} \tilde{d}(t) &= \lim_{t\to\infty} (x_{n+1} - z_{n+1}) = \lim_{s\to 0} s(1 - H(s))w(s) \\ &= \lim_{s\to 0} \frac{s^n + l_1 s^{n-1} + \cdots + l_n}{s^{n+1} + l_1 s^n + \cdots + l_n s + l_{n+1}} s^2 w(s). \end{aligned} \tag{5}$$

From Eq. (5), it can be found that if $w(t)$ is a constant disturbance, then $w(s) = \frac{1}{s}$ and $\lim_{t\to\infty} \tilde{d}(t) = 0$. Otherwise, there exists an estimation error, or the system even diverges. The estimation error can also be analyzed in the time domain.

By defining the estimation error of ESO as $\boldsymbol{e} = \boldsymbol{z} - \boldsymbol{x}$, the dynamic equation of $\boldsymbol{e}$ is described as:

$$\dot{\boldsymbol{e}} = (A - LC)\boldsymbol{e} - Eh. \tag{6}$$

When the system is in the steady state, the system states have converged to the equilibrium point. Then, the component of perturbation h that relies on the system states can be regarded as a constant. Thus, the component that relies on the external disturbance w will have a persistent influence on the control system. Three situations with different external disturbances can be analyzed as follows:

1. When the disturbance satisfies $\frac{\mathrm{d}w(t)}{\mathrm{d}t} = 0$, Eq. (6) turns to $\dot{\boldsymbol{e}} = (A - LC)\boldsymbol{e}$. Since $(A - LC)$ is a Hurwitz matrix according to the definition of A, L and C, the estimation error can converge to 0 exponentially.
2. When the disturbance satisfies $\frac{\mathrm{d}w(t)}{\mathrm{d}t} = \text{Constant}$, the equilibrium point of Eq. (6) is $\boldsymbol{e}_0 = (A - LC)^{-1} E \frac{\mathrm{d}w(t)}{\mathrm{d}t}$. At this time, there exists a constant error of the estimation of ESO. The observation error is proportional to $|\frac{\mathrm{d}w(t)}{\mathrm{d}t}|$, is inversely proportional to the bandwidth of ESO.
3. For the other kinds of disturbances, $\frac{\mathrm{d}w(t)}{\mathrm{d}t}$ is a time-varying signal, the observation error $\boldsymbol{e}$ can only converge in a compact set, whose bound relies on the upper bound of $|\frac{\mathrm{d}w(t)}{\mathrm{d}t}|$ and the bandwidth of ESO.

According to the above analysis, the time-varying disturbance will have a significant influence on the control performance. In some cases, the model of the equivalent disturbance can be obtained, it is necessary for an observer to estimate the component with known model thoroughly to increase the control accuracy.

3. Generalized ESO based control system design

The control structure is shown in Fig. 1. By introducing the disturbance dynamics into account, the generalized ESO is proposed to estimate the equivalent disturbance and system states. Thus, the outer loop state feedback controller is designed for desired tracking performance.

In this section, the controlled object is first reconstructed based on the disturbance dynamics. With the investigation of the system observability, the generalized ESO is thus proposed. Finally, the controller is designed and closed-loop stability is analyzed.

3.1. System reconstruction

Consider the SISO nonlinear system with uncertainties:

$$\begin{cases} \dot{\boldsymbol{x}} = A\boldsymbol{x} + B(b(\boldsymbol{x}) + a(\boldsymbol{x})u + d(t)) \\ y = C\boldsymbol{x}. \end{cases} \tag{7}$$

Assume that the nominal values of the scalar functions $a(\cdot)$ and $b(\cdot)$ are $\hat{a}(\cdot)$ and $\hat{b}(\cdot)$, respectively, which satisfy

$$\Delta_a(\boldsymbol{x}) = a(\boldsymbol{x}) - \hat{a}(\boldsymbol{x}), \quad \Delta_b(\boldsymbol{x}) = b(\boldsymbol{x}) - \hat{b}(\boldsymbol{x}).$$

where $\hat{a}(\cdot)$ and $\hat{b}(\cdot)$ are locally Lipschitz, with the Lipschitz constants of ℓ_a and ℓ_b, and $\hat{a}(\cdot)$ is non-singular.

Then, the system can be represented as

$$\begin{cases} \dot{\boldsymbol{x}} = A\boldsymbol{x} + B\left(\hat{b}(x) + \hat{a}(\boldsymbol{x})u + D(\boldsymbol{x}, d)\right) \\ y = C\boldsymbol{x}, \end{cases} \tag{8}$$

where $D(\cdot) \in \mathbb{R}$ is the equivalent disturbance caused by both internal uncertainty and external disturbance.

For the SISO nonlinear system in (8), the traditional ADRC methodology can be applied for observer and controller design directly. However, from the analysis above, traditional ESO cannot eliminate the disturbance with known model effectively. This is because its system reconstruction strategy cannot use the prior information effectively for ESO implementation. Eq. (6) shows that the observation accuracy of ESO depends on the upper bound of $\|h\|$, while the upper bound of $\|h\|$ reflects the uncertainty of the system. The essence of system reconstruction strategy is the process of decreasing the disturbance term h.

A system reconstruction strategy is proposed to solve the above problem. We establish the model of equivalent disturbance, based on which the system is reconstructed according to the prior information as far as possible. Assume that the equivalent disturbance in Eq. (8) satisfies:

$$\begin{cases} \dot{\boldsymbol{\theta}} = \boldsymbol{p}(\boldsymbol{\theta}) + \boldsymbol{q}(\boldsymbol{\theta})\mu \\ D = g(\boldsymbol{\theta}), \end{cases} \tag{9}$$

where $\boldsymbol{\theta} \in \mathbb{R}^m$ is system state of the disturbance system and $\mu \in \mathbb{R}$ is the input. $\boldsymbol{p} \subseteq \mathbb{R}^m \to \mathbb{R}^m$ and $\boldsymbol{q} \subseteq \mathbb{R}^m \to \mathbb{R}^m$ are two smooth vector fields. $g \subseteq \mathbb{R}^m \to \mathbb{R}$ is a smooth map. The input p is a function of external disturbance d and system state $\boldsymbol{x}$. The relative order of the disturbance system satisfies $r \le n-1$.

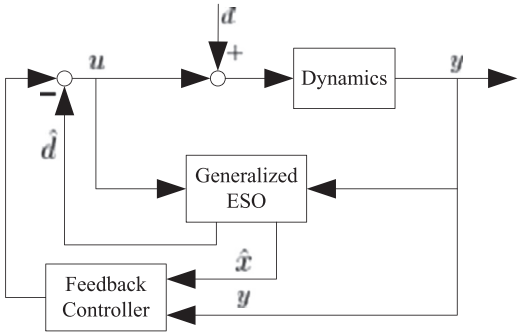

Fig. 1. Control structure of ESO based controller.

The Lie derivative of a scalar field g along a vector field $\boldsymbol{p}$ is defined by the scalar product $L_{\boldsymbol{p}}g(\boldsymbol{\theta}) = \langle \mathrm{d}g(\boldsymbol{\theta}), \boldsymbol{p}(\boldsymbol{\theta}) \rangle$, where d$g$ denotes the gradient of g. Iterated Lie derivatives are defined by $L_{\boldsymbol{p}}^k g(\boldsymbol{\theta}) = L_{\boldsymbol{p}}(L_{\boldsymbol{p}}^{k-1} g(\boldsymbol{\theta}))$.

Since the system relative order of Eq. (9) is $r \le n-1$, we get:

$$\begin{cases} L_{\boldsymbol{q}} L_{\boldsymbol{p}}^k g(\boldsymbol{\theta}) = 0, & k = 0, \ldots, r-2, \ \forall \boldsymbol{\theta} \in \mathbb{R}^m \\ L_{\boldsymbol{q}} L_{\boldsymbol{p}}^k g(\boldsymbol{\theta}) = 0, & k = r, \ldots, n, \ \forall \boldsymbol{\theta} \in \mathbb{R}^m. \end{cases}$$

By introducing the following differential homeomorphism transformation $\boldsymbol{\xi} = \Psi(\boldsymbol{\theta})$, we obtain:

$$\xi_1 = \psi_1(\boldsymbol{\theta}) = g(\boldsymbol{\theta}), \quad \xi_2 = \psi_2(\boldsymbol{\theta}) = L_{\boldsymbol{p}} g(\boldsymbol{\theta}), \ldots,$$
$$\xi_n = \psi_n(\boldsymbol{\theta}) = L_{\boldsymbol{p}}^{n-1} g(\boldsymbol{\theta}).$$

Then the nonlinear system described in Eq. (8) can be transformed into:

$$\begin{cases} \dot{\boldsymbol{\xi}} = A_d \boldsymbol{\xi} + B_d \delta \\ y = C_d \boldsymbol{\xi}, \end{cases} \tag{10}$$

where

$$A_d = \begin{bmatrix} A_r & 0_{(r-1)\times(n-r)} \\ 0_{(n-r+1)\times r} & 0_{(n-r+1)\times(n-r)} \end{bmatrix},$$
$$A_r = \begin{bmatrix} 0 & 1 & 0 & \cdots & 0 \\ 0 & 0 & 1 & \cdots & 0 \\ \vdots & \vdots & \vdots & \ddots & \vdots \\ 0 & 0 & 0 & \cdots & 1 \end{bmatrix} \in \mathbb{R}^{(r-1)\times r},$$
$$B_d = \begin{bmatrix} 0_{(r-1)\times 1} \\ I_{(n-r+1)\times 1} \end{bmatrix}, \quad C_d = [1\ 0\ \ldots\ 0],$$
$$\delta = L_{\boldsymbol{q}} L_{\boldsymbol{p}}^{r-1} g(\Psi^{-1}(\boldsymbol{\xi})) + L_{\boldsymbol{p}}^r g(\Psi^{-1}(\boldsymbol{\xi}))\mu.$$

Considering both system model in Eq. (8) and disturbance model in Eq. (9), define the generalized states of the system as $\overline{\boldsymbol{x}} = \left[\boldsymbol{x}^{\mathrm{T}} \ \boldsymbol{\xi}^{\mathrm{T}}\right]^{\mathrm{T}}$, the generalized system model can be obtained as:

$$\begin{cases} \dot{\overline{\boldsymbol{x}}} = \underbrace{\begin{bmatrix} A & BC_d \\ 0 & A_d \end{bmatrix}}_{\overline{A}} \overline{\boldsymbol{x}} + \underbrace{\begin{bmatrix} B \\ 0 \end{bmatrix}}_{\overline{B}} (\hat{b}(\overline{\boldsymbol{x}}) + \hat{a}(\boldsymbol{x})u) + \underbrace{\begin{bmatrix} 0 \\ B_d \end{bmatrix}}_{\overline{E}} \delta \\ y = \underbrace{[C\ 0]}_{\overline{C}_m} \overline{\boldsymbol{x}} \\ D = \underbrace{[0\ C_d]}_{\overline{C}_d} \overline{\boldsymbol{x}}, \boldsymbol{x} = \underbrace{[I_{n\times n}\ 0]}_{\overline{C}_x} \overline{\boldsymbol{x}}. \end{cases} \tag{11}$$

Assumption 1. For the disturbance model in Eq. (9), the input δ satisfies:

$$\|\delta\| \le k_1 + k_2 \|\overline{\boldsymbol{x}}\|,$$

where k_1 and k_2 are positive constants.

Remark 1. Similar assumption can be seen in [17].

Theorem 1. *For the reconstructed system shown in Eq. (11), the system state $\boldsymbol{x}$ is observable if and only if the system in Eq. (7) is observable.*

Proof. The Gram matrix criterion is employed to investigate the observability. For the system state $\overline{\boldsymbol{x}}$, its Gram matrix is defined as:

$$W_{\boldsymbol{x}}[0, t_1] = \int_0^{t_1} e^{\overline{A}^{\mathrm{T}} t} \overline{C}_m^{\mathrm{T}} \overline{C}_m e^{\overline{A} t} \, \mathrm{d}t,$$

where

$$e^{\overline{A}^{\mathrm{T}} t} = I_{(n+m)} + \overline{A}^{\mathrm{T}} t + \frac{(\overline{A}^{\mathrm{T}})^2 t^2}{2!} + \frac{(\overline{A}^{\mathrm{T}})^3 t^3}{3!} + \cdots$$

$$= \begin{bmatrix} I_n + A^{\mathrm{T}}t + \frac{(A^{\mathrm{T}})^2t^2}{2!} + \frac{(A^{\mathrm{T}})^3t^3}{3!} + \cdots & 0 \\ * & I_m + A_d^{\mathrm{T}}t + \frac{(A_d^{\mathrm{T}})^2t^2}{2!} + \frac{(A_d^{\mathrm{T}})^3t^3}{3!} + \cdots \end{bmatrix}$$

$$e^{\overline{A}t} = I_{(n+m)} + \overline{A}t + \frac{(\overline{A}^2t^2)}{2!} + \frac{(\overline{A}^3t^3)}{3!} + \cdots$$

$$= \begin{bmatrix} ceI_n + At + \frac{A^2t^2}{2!} + \frac{A^3t^3}{3!} + \cdots & * \\ 0 & I_m + A_dt + \frac{A_d^2t^2}{2!} + \frac{A_d^3t^3}{3!} + \cdots \end{bmatrix}$$

Then, it can be obtained that:

$$W_{\boldsymbol{x}}[0,t_1] = \int_0^{t_1} e^{\overline{A}^{\mathrm{T}}t}[C\ 0]^{\mathrm{T}}[C\ 0]e^{\overline{A}t}\,\mathrm{d}t = \int_0^{t_1} \left(1 + A^{\mathrm{T}}t + \frac{(A^{\mathrm{T}})^2t^2}{2!} + \cdots\right) C^{\mathrm{T}}C \times \left(1 + A^{\mathrm{T}}t + \frac{(A^{\mathrm{T}})^2t^2}{2!} + \cdots\right)\mathrm{d}t = \int_0^{t_1} e^{A^{\mathrm{T}}t}C^{\mathrm{T}}Ce^{At}\,\mathrm{d}t.$$

Since the system in Eq. (7) is observable, $\int_0^{t_1} e^{A^{\mathrm{T}}t}C^{\mathrm{T}}Ce^{At}\,\mathrm{d}t$ is nonsingular. It can be concluded that the reconstructed system is shown in Eq. (11), and the system state $\boldsymbol{x}$ is observable if and only if the system in Eq. (7) is observable.□

Remark 2. Comparing with the reconstructed methodology of traditional ESO scheme, the proposed system reconstruction takes the model of equivalent disturbance into account, which is more precise.

3.2. Observer design and stability analysis

From the reconstructed system model in Eq. (11), the observer is designed as follows:

$$\begin{cases} \dot{\hat{\overline{\boldsymbol{x}}}} = \overline{A}\hat{\overline{\boldsymbol{x}}} + \overline{B}(\hat{b}(\hat{\boldsymbol{x}}) + \hat{a}(\hat{\boldsymbol{x}})u) + L(y - \hat{y}) \\ \hat{y} = \overline{C}_m\hat{\overline{\boldsymbol{x}}}, \hat{\boldsymbol{x}} = \overline{C}_x\hat{\overline{\boldsymbol{x}}}, \end{cases} \tag{12}$$

where L is the observer gain to be designed, the state of the observer is defined as $\hat{\overline{\boldsymbol{x}}} = \left[\hat{\boldsymbol{x}}^{\mathrm{T}}\ \hat{\boldsymbol{\theta}}^{\mathrm{T}}\right]^{\mathrm{T}}$.

By defining the estimation error of the observer as $\boldsymbol{e} = \hat{\overline{\boldsymbol{x}}} - \overline{\boldsymbol{x}}$, we have the following equation:

$$\dot{\boldsymbol{e}} = (\overline{A} - L\overline{C}_m)\boldsymbol{e} - \overline{E}\delta + \Delta(\boldsymbol{x}, \hat{\boldsymbol{x}}), \tag{13}$$

where $\Delta(\boldsymbol{x}, \hat{\boldsymbol{x}}) = \hat{b}(\hat{\boldsymbol{x}}) - \hat{b}(\boldsymbol{x}) + (\hat{a}(\hat{\boldsymbol{x}}) - \hat{a}(\boldsymbol{x}))u$. The observer gain L is selected such that $(\overline{A} - L\overline{C}_m)$ is a Hurwitz matrix.

From (13) we can find that the estimation accuracy is determined by the bandwidth of the ESO and the perturbation term δ. Thus, there are two ways to increase the estimation accuracy of the ESO. The first way is to increase the bandwidth of the ESO. However, the bandwidth is usually limited by the robustness and measurement noise. The second way is to decrease the perturbation term δ. Both the proposed reconstruction strategy and the high order ESO in [22] are aiming at decreasing the perturbation term δ. In a word, the basis of these two methods is to decrease the uncertainty by using different nominal models. The difference is that for the proposed control strategy, the equivalent disturbance model can be used for ESO implementation, which makes the design procedure more flexible. However, the high order ESO can only adjust the order of ESO.

Remark 3. In [19,20,13,15], if the system uncertainty is assumed to be bounded directly, then it can be concluded that the estimation error is bounded. However, in most applications, the perturbation component δ not only depends on external disturbance, but also relies on internal states of the system. At this time, the convergence of the observer should be analyzed in combination with the outer loop controller.

By taking the states and disturbance estimation of the observer into account, we define a target system of controlled object described by Eq. (8):

$$\dot{\hat{\boldsymbol{x}}} = A\hat{\boldsymbol{x}} + B(\hat{b}(\hat{\boldsymbol{x}}) + \hat{a}(\hat{\boldsymbol{x}})u + C_d\hat{\boldsymbol{\theta}}). \tag{14}$$

Assumption 2. For the nonlinear system described in Eq. (14), there exists a controller $u = \beta(t, y_{\mathrm{d}}, \hat{\boldsymbol{x}}, \hat{\boldsymbol{\theta}})$ such that the system state $\boldsymbol{x}$ is globally asymptotically stable. There exists a Lyapunov function V_1 such that:

$$\frac{\partial V_1}{\partial \hat{\boldsymbol{x}}}^{\mathrm{T}}\left[A\hat{\boldsymbol{x}} + B(\hat{b}(\hat{\boldsymbol{x}}) + \hat{a}(\hat{\boldsymbol{x}})u + C_d\hat{\boldsymbol{\theta}})\right] \le -N(\hat{\boldsymbol{x}}), \quad \forall \hat{\boldsymbol{x}} \in \mathbb{R}^n, \tag{15}$$

where $N(\cdot)$ is a classical κ function, which satisfies that $\frac{\partial^2 N}{\partial \hat{\boldsymbol{x}}^2}|_{\hat{\boldsymbol{x}}} = 0$ is a positive constant. For all the system states in a compact set Ω, there exists a positive constant M such that:

$$M > \max_{\hat{\overline{\boldsymbol{x}}} \in \Omega} \|\beta(t, y_{\mathrm{d}}, \hat{\boldsymbol{x}}, \hat{\boldsymbol{\theta}})\|. \tag{16}$$

From the analysis above, we have $\lim_{t\to\infty}\hat{\boldsymbol{x}}(t) = 0$, according to the definition of observation error, we have $\boldsymbol{x} = \overline{C}_x\boldsymbol{e} + \hat{\boldsymbol{x}}$. Consequently, we only need to analyze the convergence of observation error $\boldsymbol{e}$.

Theorem 2. *Consider the nonlinear system shown in Eq. (7). Assume that the equivalent disturbance model caused by system uncertainty satisfies Assumption 1, let the observer proposed by Eq. (12), and the feedback controller under Assumption 2. Then the error of both control system and observer is bounded.*

Proof. Since the scalar functions $\hat{a}(\cdot)$ and $\hat{b}(\cdot)$ are both locally Lipschitz, the following inequality holds:

$$\|\Delta(\boldsymbol{x}, \hat{\boldsymbol{x}})\| \le \ell\|\hat{\boldsymbol{x}} - \boldsymbol{x}\| \le \ell\|\overline{C}_x\|\boldsymbol{e}, \tag{17}$$

where $\ell \triangleq \ell_a + \ell_b M$.

Since matrix $\overline{A} - L\overline{C}_m$ is Hurwitz, for any given positive definite symmetric matrix N, there exists a positive definite symmetric matrix P such that $P(\overline{A} - L\overline{C}_m) + (\overline{A} - L\overline{C}_m)^{\mathrm{T}}P = -N$. Define a Lyapunov function $V_2 = \boldsymbol{e}^{\mathrm{T}}P\boldsymbol{e}$, its time derivative is given as

$$\dot{V}_2 \le -\lambda_{\min}(N)\|\boldsymbol{e}\|^2 + 2\ell\|P\|\|\overline{B}\|\|\overline{C}_x\|\|\boldsymbol{e}\|^2 + 2\|P\|\|\overline{E}\|\|\overline{C}_x\|\|\boldsymbol{e}\|^2 + 2\|P\overline{E}\|\|\boldsymbol{e}\|(k_1 + k_2\|\hat{\boldsymbol{x}}\|) \le -c_2\|\boldsymbol{e}\|^2 + c_3\|\hat{\boldsymbol{x}}\|^2 + c_4\|\boldsymbol{e}\|, \tag{18}$$

where

$$\begin{cases} c_2 = \dfrac{\lambda_{\min}(N) - (2\ell\|\overline{B}\| - 2k_1\|\overline{E}\|)\|\overline{C}_x\|\|P\|}{2} \\ c_3 = \dfrac{2(k_2\|P\overline{E}\|)^2}{\lambda_{\min}(N) - (2\ell\|\overline{B}\| - 2k_1\|\overline{E}\|)\|\overline{C}_x\|\|P\|} \\ c_4 = 2k_1\|P\overline{E}\|. \end{cases}$$

Consider the Lyapunov function candidate

$$V(\hat{\boldsymbol{x}}, \boldsymbol{e}) = \int_0^{V_1(\hat{\boldsymbol{x}})} \gamma(s)\,\mathrm{d}s + V_2(\boldsymbol{e}).$$

Since the feedback controller u can stabilize the target system asymptotical, from converse Lyapunov theorem, there exist κ_∞ functions $\alpha_1(\cdot)$, $\alpha_2(\cdot)$ and $\alpha_3(\cdot)$ such that:

$$\alpha_1(\|\hat{\boldsymbol{x}}\|) \le V_1(\hat{\boldsymbol{x}}) \le \alpha_2(\|\hat{\boldsymbol{x}}\|), \quad \frac{\partial V_1}{\partial \hat{\boldsymbol{x}}}^{\mathrm{T}}\tilde{f}(\hat{\boldsymbol{x}}) \le -\alpha_3(\|\hat{\boldsymbol{x}}\|),$$

where $\tilde{f}(\hat{\boldsymbol{x}}) \triangleq A\hat{\boldsymbol{x}}+B(\hat{b}(\hat{\boldsymbol{x}})+\hat{a}(\hat{\boldsymbol{x}})u+C_d\hat{\boldsymbol{\theta}})$, and according to Assumption 2, we have $\alpha_3(r) \geq c_5 r^2$ holds for $c_5>0$.

For a κ function $\tilde{\gamma}(\cdot)$ that satisfies $\tilde{\gamma}(\|\hat{\boldsymbol{x}}\|) \geq c_5(c_1+c_3)\|\hat{\boldsymbol{x}}\|^2/\alpha_3(\|\hat{\boldsymbol{x}}\|)$, by selecting $\gamma(\cdot)=\tilde{\gamma}(\alpha_1^{-1}(\cdot))$, we can get the time derivative of $V(\hat{\boldsymbol{x}},\boldsymbol{e})$ as:

$$\begin{aligned}\dot{V}(\hat{\boldsymbol{x}},\boldsymbol{e}) &\leq -\gamma(\alpha_1(\|\hat{\boldsymbol{x}}\|))\alpha_3(\|\hat{\boldsymbol{x}}\|)-c_2\|\boldsymbol{e}\|^2+c_3\|\hat{\boldsymbol{x}}\|^2+c_4\|\boldsymbol{e}\| \\ &\leq -c_1\|\hat{\boldsymbol{x}}\|^2-c_2\|\boldsymbol{e}\|^2+c_4\|\boldsymbol{e}\|. \end{aligned} \tag{19}$$

From the above inequality, $\dot{V}$ is strictly negative if $\|\boldsymbol{e}\| \geq c_4/c_2$. Thus, the upper bound of observation error $\boldsymbol{e}$ is c_4/c_2. Since $\lim_{t\to\infty}\hat{\boldsymbol{x}}(t)=0$, the system state $\boldsymbol{x}$ is bounded according to the definition of observation error.□

4. Simulation results

In this section, simulation on a second-order mechanical system is employed to analyze the disturbance rejection performance of the traditional ESO. Thus, the effectiveness of the proposed generalized ESO is verified. The motion control system is described as [18]:

$$\ddot{y} = -1.41\dot{y}+b(d+u), \tag{20}$$

where u, y and d are the input, output and external disturbance, respectively, $b=23.2$ is the control gain of the system. Define the system states as $x_1=y$ and $x_2=\dot{y}$, then a standard integral form can be obtained:

$$\begin{cases}\dot{x}_1 = x_2 \\ \dot{x}_2 = f(x_1,x_2,d)+b_0u \\ y = x_1,\end{cases} \tag{21}$$

where $b_0=25$ is the nominal gain of control system, $f=\left(1-\frac{b_0}{b}\right)\dot{x}_2 -1.41\frac{b_0}{b}x_2+b_0d$ is the equivalent disturbance. For a point stabilization problem, the traditional ESO can be designed as

$$\begin{cases}\dot{z}_1 = z_2-l_1(z_1-y) \\ \dot{z}_2 = z_3-l_2(z_1-y)+b_0u \\ \dot{z}_3 = -l_3(z_1-y),\end{cases} \tag{22}$$

where l_1–l_3 are the observer gains, which are selected such that the bandwidth is 15 rad/s. Different kinds of external disturbances, such as constant disturbance, sawtooth disturbance and sinusoidal disturbance, are taken into account. The estimating errors are defined as

$$e_1=x_1-z_1, \quad e_2=x_2-z_2, \quad e_3=f(x_1,x_2,d)-z_3.$$

Assume that the constant disturbance $d=1$, then, the first order time derivative of d equals 0. The first order time derivative of equivalent disturbance at steady state satisfies $\dot{f}(\cdot)=0$. Simulation result in Fig. 2 shows that traditional ESO can deal with constant external disturbance successfully without steady state error.

4.1. Sawtooth disturbance

Considering the sawtooth external disturbance with period of 5 s and amplitude of 0–2. The first order time derivative of the equivalent disturbance at steady state is a constant. It is shown in Fig. 3 that there exists a constant error with traditional ESO, and from the analysis above, the steady state error is

$$\begin{aligned} e_0 &= (A-LC)^{-1}E\frac{\mathrm{d}w(t)}{\mathrm{d}t} = \left(\begin{bmatrix}-l_1 & 1 & 0\\ -l_2 & 0 & 1\\ -l_3 & 0 & 0\end{bmatrix}\right)^{-1}\cdot\begin{bmatrix}0\\0\\1\end{bmatrix}\cdot b_0\cdot 0.4 \\ &= \begin{bmatrix}-\frac{1}{l_3}\\ -\frac{l_1}{l_3}\\ -\frac{l_2}{l_3}\end{bmatrix}\cdot b_0\cdot 0.4 = \begin{bmatrix}-0.00296\\ -0.13300\\ -2.00000\end{bmatrix}. \end{aligned} \tag{23}$$

It can be seen that the calculation results are consistent with the simulation results. In order to deal with the sawtooth disturbance, a generalized ESO is designed based on the proposed strategy

$$\begin{cases}\dot{z}_1 = z_2-l_1(z_1-y) \\ \dot{z}_2 = z_3-l_2(z_1-y)+b_0u \\ \dot{z}_3 = z_4-l_3(z_1-y) \\ \dot{z}_4 = -l_4(z_1-y),\end{cases} \tag{24}$$

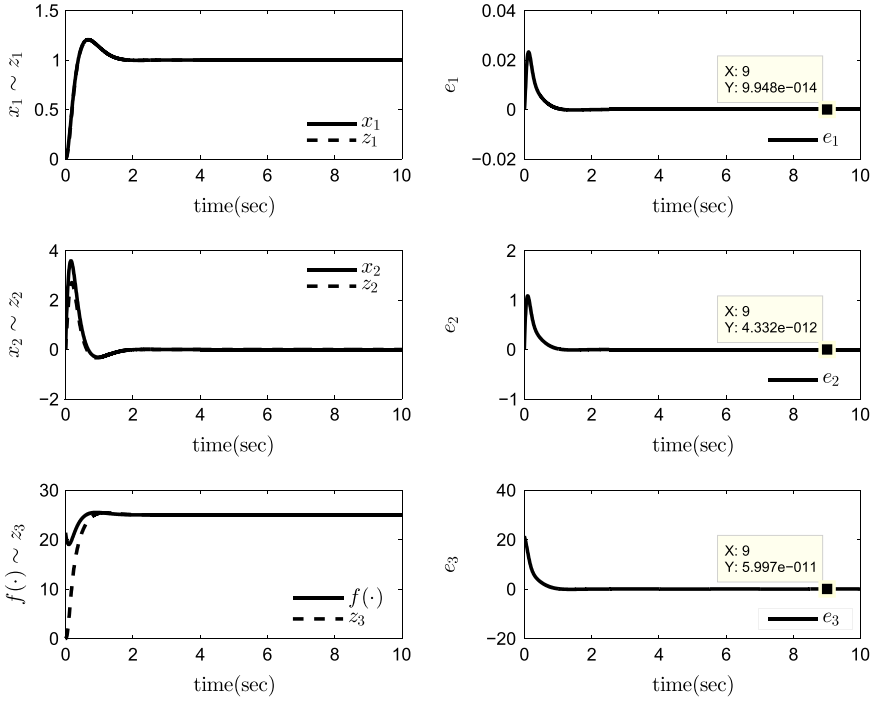

Fig. 2. Estimation performance with constant disturbance.

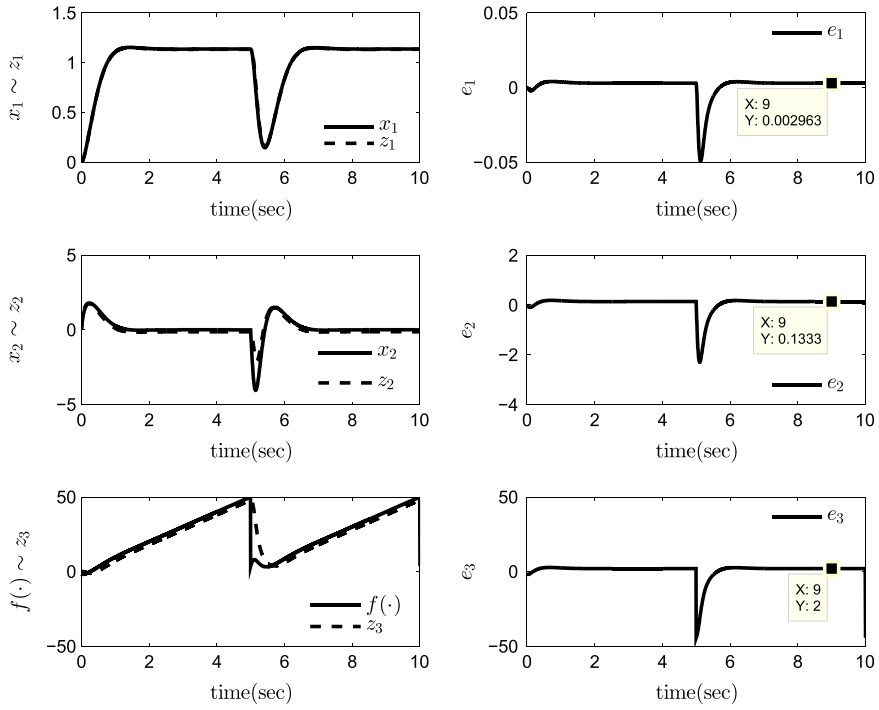

Fig. 3. Estimation performance with traditional ESO.

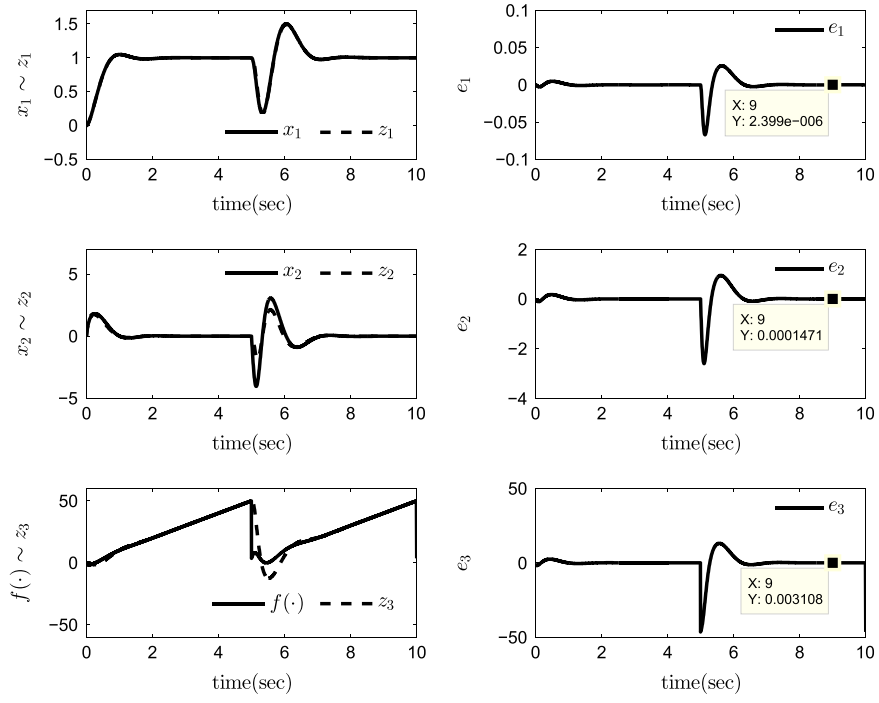

Fig. 4. Estimation performance with generalized ESO.

where the observer gains l_1–l_4 are selected such that the generalized ESO has the same cut-off frequency with traditional ESO. It is shown in Fig. 4 that with the sawtooth disturbance, the estimation error of generalized ESO can converge to 0 asymptotically.

4.2. Sinusoidal disturbance

Considering the sinusoidal external disturbance with period of 2π s and amplitude of 0.5. The first order time derivative of external disturbance is periodic signal. Using the similar calculation method, we get the peak estimation error of traditional ESO as $[0.0074\ 0.3333\ 5.0000]^{\mathrm{T}}$, which can be verified in Fig. 5. To deal with sinusoidal external disturbance, the proposed strategy is employed to design the following generalized ESO as:

$$\begin{cases} \dot{z}_1 = z_2 - l_1(z_1 - y) \\ \dot{z}_2 = z_3 - l_2(z_1 - y) + b_0 u \\ \dot{z}_3 = z_4 - l_3(z_1 - y) \\ \dot{z}_4 = -\omega_0^2 z_3 + z_5 - l_4(z_1 - y) \\ \dot{z}_5 = -l_5(z_1 - y), \end{cases} \tag{25}$$

where the observer gains l_1–l_5 are selected such that the

generalized ESO has the same cut-off frequency with traditional ESO. It is also shown in Fig. 6 that with the sinusoidal disturbance, estimation error of generalized ESO can converge to 0 asymptotically.

4.3. Case study of nonlinear system

Although the proposed ESO is designed in linear form, it can also deal with the nonlinear control problem. A nonlinear system is given as

$$\ddot{y} = -1.41\dot{y} + 23.2d + y\dot{y} + 0.2e^{y} + 23.2u, \tag{26}$$

Define the system states as $x_1 = y$ and $x_2 = \dot{y}$, then a standard integral form can be obtained:

$$\begin{cases} \dot{x}_1 = x_2 \\ \dot{x}_2 = f(x_1, x_2, d) + b_0 u \\ y = x_1, \end{cases} \tag{27}$$

where $b_0 = 25$ is the nominal gain of control system, $f = \left(1 - \frac{b_0}{b}\right)\dot{x}_2 - 1.41\frac{b_0}{b}x_2 + x_1x_2 + 0.2e^{x_1} + b_0 d$ is the equivalent disturbance. The proposed strategy is compared with the traditional ESO design method and high order ESO proposed in [22].

Figs. 7 and 8 are the comparison of control effect and estimation error for nonlinear system. It is shown by the results that, although the proposed ESO is designed under linear form, it can successfully deal with the nonlinear control problem. Comparing with traditional ESO, the high order ESO proposed in [22] can obtain higher estimating accuracy. However, periodic estimation error still exists. However, the estimation error of proposed strategy can converge to 0 by introducing the disturbance dynamics into ESO design procedure. Thus, the proposed strategy can obtain higher control accuracy for nonlinear systems with fast time-varying disturbances.

Here, fast time-varying disturbances with period of 0.4π s is considered in the simulation. Fig. 9 shows the estimation effect of proposed strategy and high order ESO in [22]. It is shown that the proposed strategy can obtain better estimation accuracy comparing with high order ESO.

5. Applications and experiments

5.1. System model

In this section, attitude tracking control problem of an aircraft is employed to show the effectiveness of the proposed strategy.

By choosing modified Rodrigues parameters (MRPs) as the attitude representations, the attitude tracking error model is described as follows [23]:

$$\begin{cases} \dot{\tilde{\boldsymbol{\sigma}}} = G(\tilde{\boldsymbol{\sigma}})\tilde{\boldsymbol{\omega}} \\ \dot{\tilde{\boldsymbol{\omega}}} = J^{-1}[-(\tilde{\boldsymbol{\omega}} + \tilde{R}\boldsymbol{\omega}_{\mathrm{d}}) \times J(\tilde{\boldsymbol{\omega}} + \tilde{R}\boldsymbol{\omega}_{\mathrm{d}}) + F\boldsymbol{u} + \boldsymbol{d}] - (\tilde{R}\dot{\boldsymbol{\omega}}_{\mathrm{d}} - [\tilde{\boldsymbol{\omega}}\times]\tilde{R}\boldsymbol{\omega}_{\mathrm{d}}), \end{cases} \tag{28}$$

where $J \in \mathbb{R}^{3\times 3}$ is a symmetric square positive definite inertia matrix, F is the input matrix, $F\boldsymbol{u}$ is the control torque, $\boldsymbol{d}$ is the external disturbance. $\tilde{\boldsymbol{\sigma}}$, $\tilde{\boldsymbol{\omega}}$ and $\tilde{R}$ are, respectively, MRPs, angular velocity and attitude transition matrix error defined as:

$$\tilde{\boldsymbol{\sigma}} = \boldsymbol{\sigma} \oplus \boldsymbol{\sigma}_{\mathrm{d}}^{-1}, \quad \tilde{\boldsymbol{\omega}} = \boldsymbol{\omega} - \tilde{R}\boldsymbol{\omega}_{\mathrm{d}}, \quad \tilde{R} = RR_{\mathrm{d}}^{\mathrm{T}}. \tag{29}$$

From Eq. (28), we can obtain:

$$\ddot{\tilde{\boldsymbol{\sigma}}} = \overline{G}(\tilde{\boldsymbol{\sigma}}, \dot{\tilde{\boldsymbol{\sigma}}})G^{-1}(\tilde{\boldsymbol{\sigma}})\dot{\tilde{\boldsymbol{\sigma}}} + G(\tilde{\boldsymbol{\sigma}})\dot{\tilde{\boldsymbol{\omega}}}, \tag{30}$$

where $\overline{G}(\tilde{\boldsymbol{\sigma}}, \dot{\tilde{\boldsymbol{\sigma}}})$ is the time derivative of $G(\tilde{\boldsymbol{\sigma}})$. Define the system states as $\boldsymbol{x}_1 = \tilde{\boldsymbol{\sigma}}$, $\boldsymbol{x}_2 = \dot{\tilde{\boldsymbol{\sigma}}}$. Assume that the nominal values of inertia matrix and input matrix are J_0 and F_0, respectively, with their errors defined as $\Delta J = J - J_0$ and $\Delta F = F - F_0$. We can use the feedback linearization

$$\boldsymbol{u} = F_0^{-1}J_0G^{-1}(\tilde{\boldsymbol{\sigma}})\left(\boldsymbol{v} - \overline{G}(\tilde{\boldsymbol{\sigma}}, \dot{\tilde{\boldsymbol{\sigma}}})G^{-1}(\tilde{\boldsymbol{\sigma}})\dot{\tilde{\boldsymbol{\sigma}}}\right) + F_0^{-1}L(\tilde{\boldsymbol{\omega}} + \tilde{R}\boldsymbol{\omega}_{\mathrm{d}})J_0^{*} + F_0^{-1}J_0(\tilde{R}\dot{\boldsymbol{\omega}}_{\mathrm{d}} - [\tilde{\boldsymbol{\omega}}\times]\tilde{R}\boldsymbol{\omega}_{\mathrm{d}}), \tag{31}$$

to reduce the system dynamics to $\ddot{\tilde{\boldsymbol{\sigma}}} = \boldsymbol{v} + \boldsymbol{f}$, where $L(\cdot)$ and $\mathrm{vec}(\cdot)$ satisfy $L(\tilde{\boldsymbol{\omega}} + \tilde{R}\boldsymbol{\omega}_{\mathrm{d}})\mathrm{vec}(J_0) = (\tilde{\boldsymbol{\omega}} + \tilde{R}\boldsymbol{\omega}_{\mathrm{d}}) \times J_0(\tilde{\boldsymbol{\omega}} + \tilde{R}\boldsymbol{\omega}_{\mathrm{d}})$. The system uncertainty is described as

$$\boldsymbol{f} = -J_0^{-1}F_0[\delta\dot{\tilde{\boldsymbol{\omega}}} + L(\tilde{\boldsymbol{\omega}} + \tilde{R}\boldsymbol{\omega}_{\mathrm{d}})\mathrm{vec}(\delta) + \delta(\tilde{R}\dot{\boldsymbol{\omega}}_{\mathrm{d}} - [\tilde{\boldsymbol{\omega}}\times]\tilde{R}\boldsymbol{\omega}_{\mathrm{d}}) - \boldsymbol{d}], \tag{32}$$

where $\delta \triangleq (FF_0)^{-1}(F_0\Delta J - \Delta F J_0)$.

When the desired MRPs are sinusoidal signal, correspondingly, $\boldsymbol{\omega}_{\mathrm{d}}$ and $\dot{\boldsymbol{\omega}}_{\mathrm{d}}$ are sinusoidal signals with same period. The system states remain almost time invariant when the system converges to steady state such that $\tilde{\boldsymbol{\sigma}} \approx 0$, $\tilde{\boldsymbol{\omega}} \approx 0$, $\dot{\tilde{\boldsymbol{\omega}}} \approx 0$ and $\tilde{R} \approx I_3$. At this time,

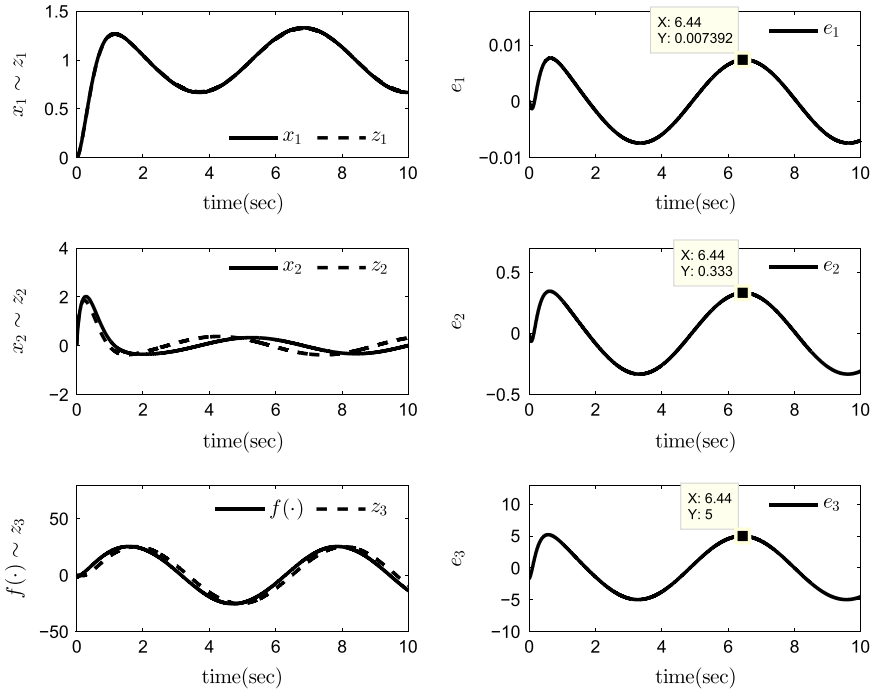

Fig. 5. Estimation performance with traditional ESO.

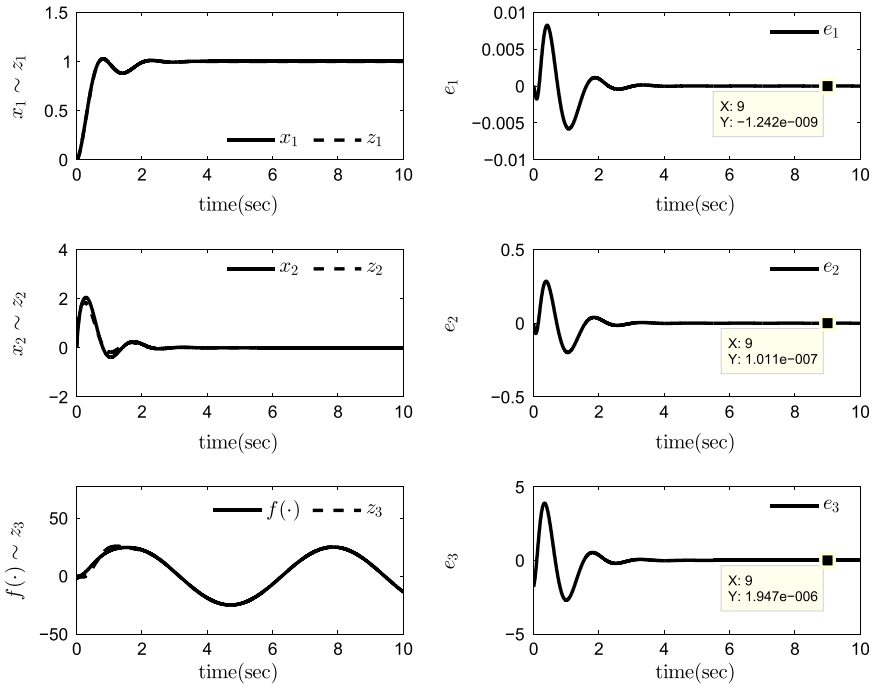

Fig. 6. Estimation performance with generalized ESO.

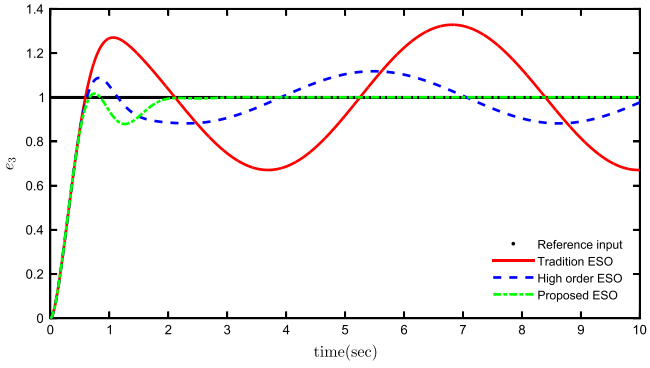

Fig. 7. Control effect comparison with difference ESOs.

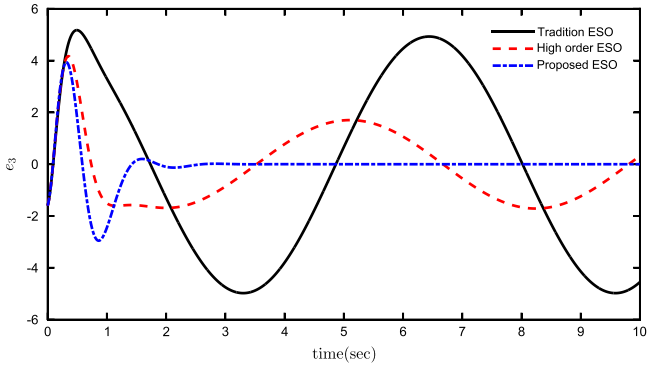

Fig. 8. Estimation effect comparison for nonlinear system.

the system uncertainty can be rewritten as

$$\boldsymbol{f} \approx -J_0^{-1}F_0\left[L(\boldsymbol{\omega}_\mathrm{d})\delta^* + \delta\dot{\boldsymbol{\omega}}_\mathrm{d} - \boldsymbol{d}\right]. \tag{33}$$

It is clearly that the system suffers from a periodic disturbance at steady state. Assuming that the period of the desired MRPs is T_0,

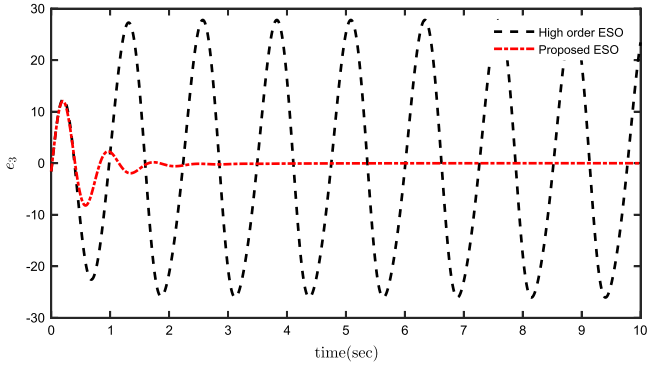

Fig. 9. Estimation effect comparison with fast time-varying disturbance.

thus the equivalent disturbance can be modeled as

$$\begin{cases} \dot{\boldsymbol{\theta}}_i = \begin{bmatrix} 0 & 1 & 0 \\ -\omega_0^2 & 0 & 1 \\ 0 & 0 & 0 \end{bmatrix}\boldsymbol{\theta}_i + \begin{bmatrix} 0 \\ 0 \\ 1 \end{bmatrix}\boldsymbol{h}_i(t), & \omega_0 = \dfrac{2\pi}{T_0} \\ \boldsymbol{f}_i = [1\ 0\ 0]\boldsymbol{\theta}_i, & i = 1,2, \end{cases} \tag{34}$$

where $i = 1, 2$ are the nick and roll axis of the aircraft, respectively.

5.2. Control system implementation

The attitude heading reference system (AHRS) can provide both attitude and angular velocity. However, these measurements are usually affected by the noise and constant (or slowly time-varying) bias. To decrease these influences, we define the generalized observation error

$$\boldsymbol{e} = \mu(\tilde{\boldsymbol{\sigma}} - \hat{\boldsymbol{z}}_1) + (1-\mu)(\dot{\tilde{\boldsymbol{\sigma}}} - \hat{\boldsymbol{z}}_2), \tag{35}$$

where $0 < \mu < 1$ is a constant, $\hat{\boldsymbol{z}}_1$ and $\hat{\boldsymbol{z}}_2$ are the estimation of $\tilde{\boldsymbol{\sigma}}$ and $\dot{\tilde{\boldsymbol{\sigma}}}$, respectively. The measurements can be acquired by Eq. (29) and $\dot{\tilde{\boldsymbol{\sigma}}} = G^{-1}(\tilde{\boldsymbol{\sigma}})\tilde{\boldsymbol{\omega}}$. By using the proposed strategy in this paper,

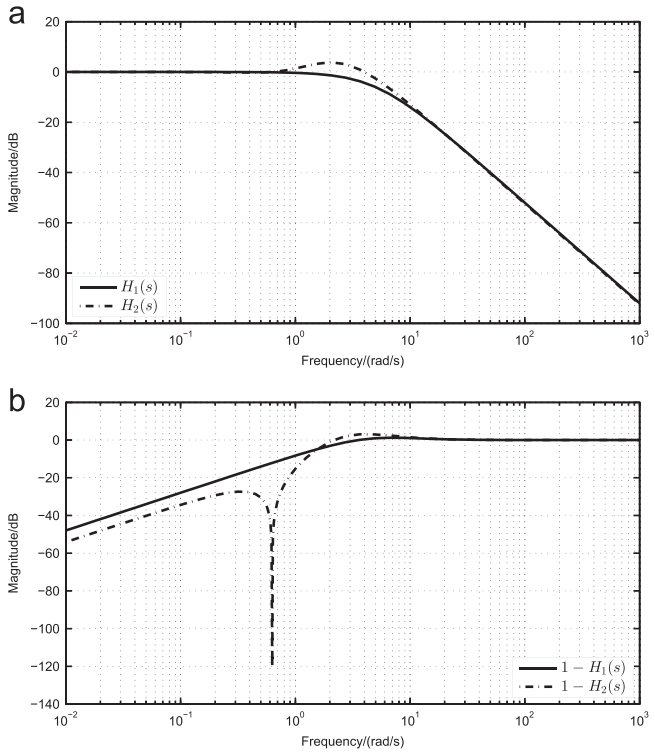

Fig. 10. Frequency response of equivalent filter. (a) Frequency responses of $H(s)$. (b) Frequency responses of $1-H(s)$.

the ESO is proposed as

$$\begin{cases} \dot{\hat{\boldsymbol{z}}}_1 = \hat{\boldsymbol{z}}_2 + l_1\boldsymbol{e} \\ \dot{\hat{\boldsymbol{z}}}_2 = \boldsymbol{v} + \hat{\boldsymbol{z}}_3 + l_2\boldsymbol{e} \\ \dot{\hat{\boldsymbol{z}}}_3 = \hat{\boldsymbol{z}}_4 + l_3\boldsymbol{e} \\ \dot{\hat{\boldsymbol{z}}}_4 = -\omega_0^2\hat{\boldsymbol{z}}_3 + \hat{\boldsymbol{z}}_5 + l_4\boldsymbol{e} \\ \dot{\hat{\boldsymbol{z}}}_5 = l_5\boldsymbol{e}, \end{cases} \tag{36}$$

where l_1–l_5 should make the matrix $\overline{A}-L\overline{C}_m$ a Hurwitz matrix. Then, the controller $\boldsymbol{v}$ can be simply designed as

$$\boldsymbol{v} = -k_p\boldsymbol{z}_1 - k_d\boldsymbol{z}_2 - \boldsymbol{z}_3, \tag{37}$$

where $\boldsymbol{z}_3$ is the estimated disturbance, $k_p, k_p > 0$ are the controller parameters. By substituting Eq. (37) into Eq. (31), the control input can be finally obtained.

5.3. Results and analysis

The experiment of attitude tracking is accomplished, while the desired MRPs are expressed as follows:

$$\sigma_{\mathrm{d}1} = 0.03\cos\left(\frac{\pi}{5}t+\pi\right), \quad \sigma_{\mathrm{d}2} = 0.03\sin\left(\frac{\pi}{5}t\right), \quad \sigma_{\mathrm{d}3} = 0 \tag{38}$$

The performance of proposed strategy is compared with traditional ESO. The parameters of traditional ESO are selected to make sure it has the same cut-off frequency with proposed ESO. Assuming that the equivalent filter of traditional and generalized ESOs are $H_1(s)$ and $H_2(s)$, respectively. The frequency responses of these two observers are illustrated in Fig. 10. From the frequency response of $H(s)$, the two ESOs have same cut-off frequency. It is shown that $1-H_2(s)$ is lower than $1-H_1(s)$ when the frequency is less than 1 rad/s, and $1-H_2(s)$ has a valley value at about 0.63 rad/s. Consequently, the proposed generalized ESO has better disturbance rejection performance against traditional ESO, especially at the corresponding frequency. From Eq. (33), the equivalent disturbance contains the component of signal with the period of σ. According to Eq. (38), the frequency is 0.628 rad/s, which means

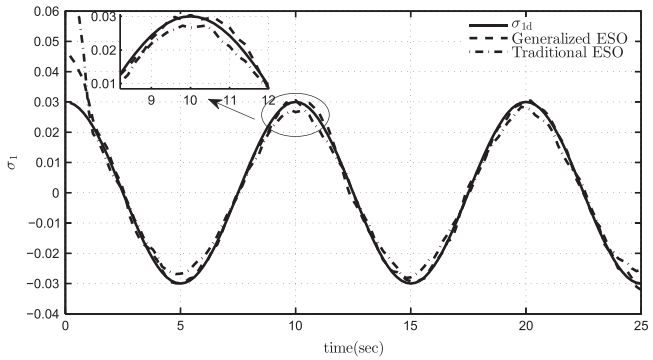

Fig. 11. Comparison of tracking control performance of roll axis.

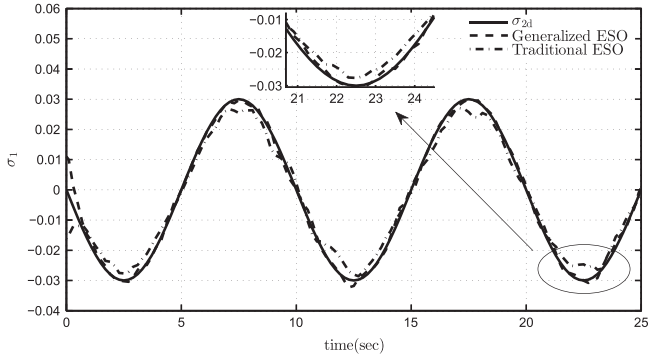

Fig. 12. Comparison of tracking control performance of pitch axis.

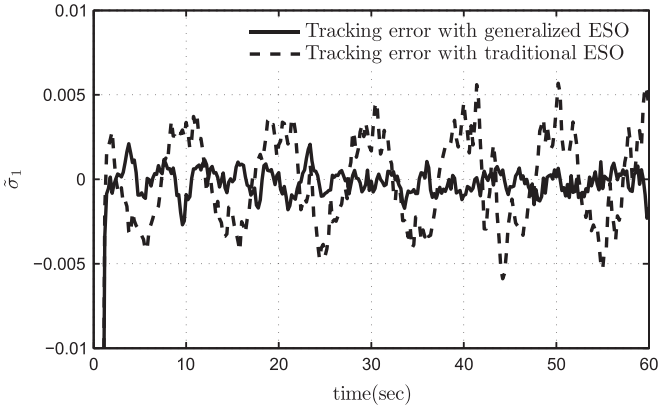

Fig. 13. Tracking error comparison of $\tilde{\sigma}_1$.

the generalized ESO can suppress the period component of the equivalent disturbance.

Figs. 11 and 12 show the tracking performance comparison of the proposed generalized ESO and traditional ESO. It is illustrated from the larger view that while the desired attitude has a maximum differential of desired angular velocity, there exists a tracking error obviously. However, the proposed generalized ESO can successfully eliminate the tracking error for the time-varying desired attitude. Fig. 13 shows the tracking error $\tilde{\sigma}_1$ of traditional and generalized ESOs. It is clearly that the tracking error is sinusoidal signal with same period as desired MRPs. This is because traditional ESO cannot suppress the time-varying component of equivalent disturbance completely. Nevertheless, since the generalized ESO has taken the model of equivalent disturbance into account, it can eliminate the periodic tracking error successfully. Table 1 shows the comparison of the attitude tracking accuracy.

Table 1
Comparison of control performance (RMS error).

Variables	σ_1	σ_2	σ_3
Without ESO	7.1×10^{-3}	7.7×10^{-3}	8.8×10^{-3}
With Traditional ESO	2.9×10^{-4}	2.6×10^{-4}	1.7×10^{-4}
With Generalized ESO	0.9×10^{-4}	1.0×10^{-4}	1.9×10^{-4}

6. Conclusions

ESO plays an important role in ADRC methodology. By analyzing the disturbance rejection performance of ESO, it is first pointed out that ESO approach is essentially the system reconstruction and state estimation of the controlled object. For traditional ESO design, the simple system reconstruction strategy makes it impossible to suppress time-varying disturbance effectively. The proposed methodology can apply the prior information of the system uncertainties as far as possible, thus the estimating accuracy can be increased. Simulations show that the proposed methodology can obtain better performance under time-varying disturbances. Experiments of attitude tracking are carried out on a quadrotor aircraft. Comparing with traditional ADRC methodology, the generalized ESO based control can eliminate the influence caused by the component of disturbance with known model thoroughly.

The proposed strategy can successfully deal with the equivalent disturbances with known model. However, it cannot identify the parameter of the disturbances online, i.e. the period of the sine disturbances. Thus, in future works, the adaptive law and learning based algorithm will be investigated to estimate the parameters of disturbances online. Meanwhile, it is shown in many researches that the bandwidth of ESO is key point that determines the performance. The parameters optimization method with constraint of bandwidth will also be under investigation. It is also known that the controller and observer design for systems with dead-zone and constraints have been widely concerned [9,24]. Thus, the ESO design for such systems will also be under investigation.

References

[1] Guo L, Cao S. Anti-disturbance control theory for systems with multiple disturbances: a survey. ISA Trans 2014;53(4):846–9.
[2] Ohnishi K. A new servo method in mechatronics. Trans Jpn Soc Electr Eng 1987;107:83–6.
[3] Han J. From PID to active disturbance rejection control. IEEE Trans Ind Electron 2009;56(3):900–6.
[4] Hur H, Ahn H-S. Unknown input H_∞ observer-based localization of a mobile robot with sensor failure. IEEE/ASME Trans Mechatron 2014;19(6):1830–8.
[5] Kwon S, Chung WK. A discrete-time design and analysis of perturbation observer for motion control applications. IEEE Trans Control Syst Technol 2003;11(3):399–407.
[6] She J-H, Fang M, Ohyama Y, Hashimoto H, Wu M. Improving disturbance-rejection performance based on an equivalent-input-disturbance approach. IEEE Trans Ind Electron 2008;55(1):380–9.
[7] Li H, Gao H, Shi P, Zhao X. Fault-tolerant control of Markovian jump stochastic systems via the augmented sliding mode observer approach. Automatica 2014;50(7):1825–34.
[8] Liu Y-J, Tong S. Adaptive fuzzy control for a class of unknown nonlinear dynamical systems. Fuzzy Sets Syst 2015;263:49–70.
[9] Liu Y-J, Tong S, Li D-J, Gao Y. Fuzzy adaptive control with state observer for a class of nonlinear discrete-time systems with input constraint. IEEE Trans Fuzzy Syst 2016. http://dx.doi.org/10.1109/TFUZZ.2015.2505088.
[10] Liu Y-J, Gao Y, Tong S, Li Y. Fuzzy approximation-based adaptive backstepping optimal control for a class of nonlinear discrete-time systems with dead-zone. IEEE Trans Fuzzy Syst 2016;24(1):16–28.
[11] Zheng Q, Gao L, Gao Z. On stability analysis of active disturbance rejection control for nonlinear time-varying plants with unknown dynamics. In: Proceedings of IEEE conference on decision and control; 2007. p. 3501–6.
[12] Su J, Qiu W, Ma H, Woo P-Y. Calibration-free robotic eye-hand coordination based on an auto disturbance-rejection controller. IEEE Trans Robot 2004;20(5):899–907.
[13] Xia Y, Zhu Z, Fu M, Wang S. Attitude tracking of rigid spacecraft with bounded disturbances. IEEE Trans Ind Electron 2011;58(2):647–59.
[14] Li S, Li J, Mo Y. Piezoelectric multi-mode vibration control for stiffened plate using ADRC-based acceleration compensation. IEEE Trans Ind Electron 2014;61(12):6892–902.
[15] Wang J, Li S, Yang J, Wu B, Li Q. Extended state observer-based sliding mode control for PWM-based DC–DC buck power converter systems with mismatched disturbances. IET Control Theory Appl 2015;9(4):579–86.
[16] Sira-Ramírez H, Linares-Flores J, García-Rodríguez C, Contreras-Ordaz MA. On the control of the permanent magnet synchronous motor: an active disturbance rejection control approach. IEEE Trans Control Syst Technol 2014;22(5):2056–63.
[17] Guo B-Z, Zhao Z-l. On the convergence of an extended state observer for nonlinear systems with uncertainty. Syst Control Lett 2011;60(6):420–30.
[18] Gao Z. Scaling and bandwidth-parameterization based controller tuning. In: Proceedings of the American control conference, vol. 6; 2006. p. 4989–96.
[19] Li S, Yang J, Chen W-H, Chen X. Generalized extended state observer based control for systems with mismatched uncertainties. IEEE Trans Ind Electron 2012;59(12):4792–802.
[20] Yao J, Jiao Z, Ma D. Adaptive robust control of DC motors with extended state observer. IEEE Trans Ind Electron 2014;61(7):3630–7.
[21] Madoński R, Herman P. Survey on methods of increasing the efficiency of extended state disturbance observers. ISA Trans 2015;56(5):18–27.
[22] Godbole AA, Kolhe JP, Talole SE. Performance analysis of generalized extended state observer in tackling sinusoidal disturbances. IEEE Trans Control Syst Technol 2013;21(6):2212–23.
[23] Wang L, Su J. Robust disturbance rejection control for attitude tracking of an aircraft. IEEE Trans Control Syst Technol 2015;23(6):2361–8.
[24] Liu Y-J, Tong S. Barrier Lyapunov functions-based adaptive control for a class of nonlinear pure-feedback systems with full state constraints. Automatica 2016;64:70–5.